Approached Evaluation of Rectangular Spiral Antenna Parameters for UHF RFID tag

MAKROUM El Mostafa, RIFI Mounir, LATRACH Mohamed, BENBASSOU Ali

***Abstract*—**: Radiofrequency identification is an emerging and promising technology for the identification of individuals and goods: the automation of manual operation, rapidity, precise information... the are many RFID technologies. In this article, we are interested in the passive UHF RFID technology and especially to the calculation of parameters of spirals rectangular antennas for RFID. First we present a model based on the theory of diffraction by fine wires, we arrive at an integro-differential equation, this equation can be solved by using the method of moments. Although this method gives us a very good agreement with the measure, it remains gourmand in calculation time. We then develop a method to simplify the calculation of the parameters of spiral antenna for RFID tag without resorting to numerical analysis methods. In high frequency, when resonances appear, we introduce the propagation using the Transmission Line Theory. Knowing that this theory doesn't take into account neither common mode currents nor lateral tracks of the loops. Then we introduce some improvements on it. These improvements consist on the one hand to integrate common mode in this theory decomposing excitations and on the other hand to correct the positions and magnitudes of resonances by introducing lateral tracks of these loops. The results obtained in this study highlight interesting prospects for future studies.

***Keywords*—** Antennas, Spiral antennas, RFID tags, UHF RFID, Method of moments, S11 parameter, Transmission Lines Theory.

I. Introduction

RADIO Frequency IDentification (RFID) is an automatic identification method, relying on storing and remotely retrieving data using devices called RFID tags or transponders. An RFID tag is a small object that can be attached to or incorporated into a product, animal or person. RFID tag contains antenna to enable it to receive and respond to Radio-Frequency (RF) queries from an RFID reader or interrogator. Passive tags require no internal power source, whereas active tags require a power source.

The trend in the automated industry is to move towards fast and real-time identification, further improving high level of accuracy needed to enable continuous identification and monitoring. Such a level of real-time knowledge is often called ambient intelligence. One of the technology that made this concept viable is known as Radio Frequency IDentification or more simply RFID. Companies, individuals and states can benefit from such a technology. There are numerous applications among which we find: logistics, access control, transportation, pets management, counterfeit struggle, e-document (biometric passport), etc. As usual with new technologies, these benefits should be balanced with the impacts on people privacy. Probably like no other technology, RFID opens new application horizons but also introduces new reflection topics for lawmakers.

Passive (or without embedded electrical energy) RFID transponders are composed of an electronic Integrated Circuit (IC) that usually contains data and an antenna. The IC is powered by a reader that also communicates with the tag in order to get its data (usually in the order of a few hundreds bits). The general overview of such a system is shown in Fig.1.

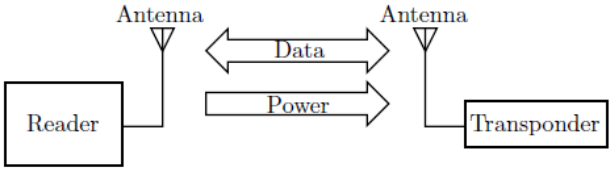

Fig.1: RFID system overview

RFID systems use mainly four frequency bands [1], [2] and [3]: 125KHz (LF band, Low Frequency), 13.56 MHz (HF, High Frequency), 860-960MHz (UHF, Ultra High frequencies), 2.45 GHz (microwave). In recent years a growing interest in the field of industry and research focused on passive UHF RFID technology. It presents a low cost solution. It also helps to have a data rate higher (around 20kbit/s) and achieve a reading range greater than other technologies called passive RFID. This interest has helped put in place in most parts of the world regulations and industry

Manuscript received November 31, 2010: Revised version received April 30, 2011. Approached Evaluation of rectangular spiral antenna parameters for UHF RFID tag.

El Mostafa MAKROUM is with the Networks Laboratory, Computer, Telecom & Multimedia, Higher School of Technology, and CED sciences de l'ingénieur – ENSEM, University Hassan II, Casablanca, Km 7, Route El Jadida, B.P. 8012 Oasis Casablanca Oasis Casablanca, Morocco, phone: 00-212-661-514-850; e-mail: elmostafa1980@hotmail.com.

Mounir RIFI is with the Networks Laboratory, Computer, Telecom & Multimedia, Higher School of Technology, University Hassan II, Casablanca, Km 7, Route El Jadida, B.P. 8012 Oasis Casablanca Oasis Casablanca, Morocco, phone: 00-212-661-414-742; e-mail: mounir@atm.com.

Mohamed LATRACH is with the Radio & Microwave Group, ESEO, Graduate School of Engineering, 4 Rue Merlet de la Boulaye, PO 30926, 49009 Angers, France, e-mail: mohamed.latrach@free.fr .

Ali BENBASSOU is with the Laboratory of Transmission and Processing of Information EMC / Telecom, Higher School of Technology PO. 2427 FES Morocco, phone: 00-212-661-220-213; e-mail: alibenbassou@yahoo.fr

standards for market development of this technology.

In the first part of this document, a brief presentation of passive RFID technology is exposed. Then the modeling of a rectangular spiral RFID antenna using the moment method and the results of simulations and measurements are discussed and presented in a second part. Then we develop a method for estimating the peak current and thus the resonant frequency of spiral antennas.

II. The Principle of Passive RFID Technology

An automatic identification application RFID, as shown in Fig. 2, consists of a base station that transmits a signal at a frequency determined to one or more RFID tags within its field of inquiry. When the tags are "awakened" by the base station, a dialogue is established according to a predefined communication protocol, and data are exchanged.

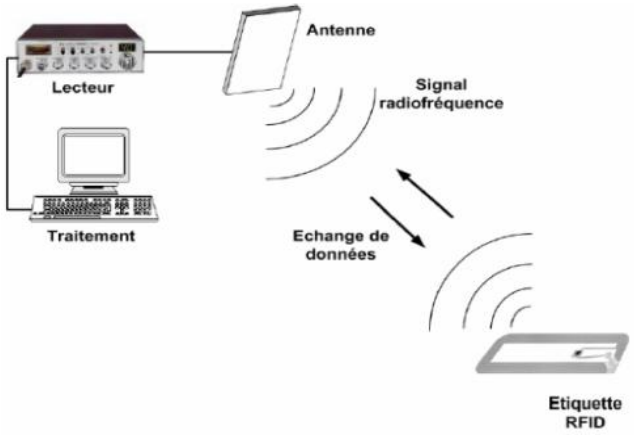

Fig.2: Schematic illustration of an RFID system

The tags are also called a transponder or tag, and consist of a microchip associated with an antenna. It is an equipment for receiving an interrogator radio signal and immediately return via radio and the information stored in the chip, such as the unique identification of a product.

Depending on the operating frequency of the coupling between the antenna of the base station and the tag may be an inductive coupling (transformer principle) or radiative (far-field operation). In both cases of coupling, the chip will be powered by a portion of the energy radiated by the base station.

To transmit the information it contains, it will create an amplitude modulation or phase modulation on the carrier frequency. The player receives this information and converts them into binary (0 or 1). In the sense reader to tag, the operation is symmetric, the reader transmits information by modulating the carrier. The modulations are analyzed by the chip and digitized.

III. Modeling of a Spiral Antenna in UHF Band

To predict the resonant frequencies of the currents induced in the antenna structures forming tags, such as spiral antennas rectangular ICs, we have used initially the model based on the theory of diffraction by thin wires [4]. We arrive at an integro-differential equation, and whose resolution is based on the method of moments [5]. Although a very good result is obtained, the computation time required is a major drawback. It is quite high. In a second step, the study is to find a method to simplify the estimation of the resonance frequency of rectangular spiral antennas in various frequency ranges.

A. Method of Moments

It is an integral analysis method used to reduce a functional relationship in a matrix relationship which can be solved by conventional techniques. It allows a systematic study and can adapt to very complex geometric shapes.

This method is more rigorous and involves a more complicated formalism leading to heavy digital development. It applies in cases where the antenna can be decomposed into one or several environments: the electromagnetic field can then be expressed as an integral surface. It implicitly takes into account all modes of radiation.

Moreover, the decomposition of surface current to basis functions, greatly simplifies the solution of integral equations which makes the method simple to implement.

This procedure is based on the following four steps:

- Derivation of integral equation.
- Conversion of the integral equation into a matrix equation.
- Evaluation of the matrix system.
- And solving the matrix equation.

B. Formulation of the method of moments [5] [6]

We have chosen the configuration shown in Fig.3, a rectangular metal track, printed on an isolating substrate. It consists of length A, width B and thickness e.

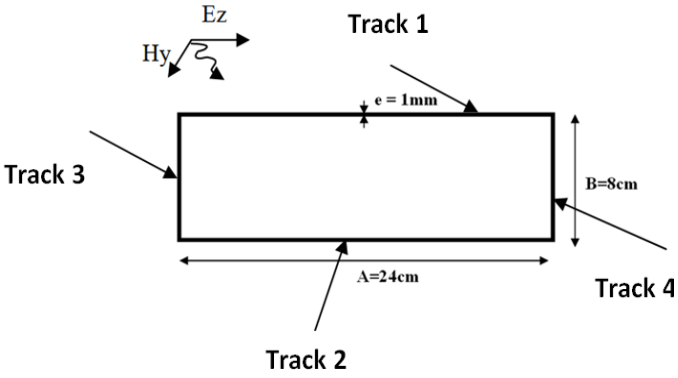

Fig.3: Dimensions of the track used in the simulation

The theory of antennas for connecting the induced current in the metal track to the incident electromagnetic field (Ei, Hi) using integro-differential equation as follows:

$$\vec{t}(l)\vec{E}^{i}(l) = j\omega\mu\int_{0}^{L} I(l')\vec{t}(l')\vec{t}(l)G(R)dl$$

$$+\frac{j}{\varepsilon\omega}\vec{t}(l)grad\vec{d}\int_{0}^{L}\vec{t}(l')grad\vec{d}I(l')G(R)dl' \quad (1)$$

The method used to solve such equations is the method of moments [4].

The problem thus is reduced to solving a linear system of the form:

$$[V] = [Z_{mn}][I] \quad (2)$$

With :

[I] represents the currents on each element of the structure.

[V.] represents the basic tension across each element m in length Δ given by:

$$Vm = Ei(m)\Delta \quad (3)$$

[Zmn] represents the generalized impedance matrix, reflecting the EM coupling between the different elements of the antenna.

The rectangular loop will be discretized into N identical segments of length Δ:

$$\Delta = 2\frac{(A+B)}{N} \quad (4)$$

The discretization step is chosen so as to ensure the convergence of the method of moments.

$$\Delta = \frac{\lambda}{20} \quad (5)$$

We conclude from this relationship that the number of segments required for convergence of numerical results is:

$$N = 40\frac{(A+B)}{\lambda} \quad (6)$$

λ : Represents the smallest wavelength of EM field incident.

The simulations will focus on frequencies between:

100MHz < f < 1.8GHz whether 17cm < λ < 3m

The number of segments will be: N = 76. The illumination of the loop is done by an plane EM wave, arriving in tangential impact such that the incident electric field Ezi is parallel to the longest track.

The amplitude of the incident field is normalized 1V/m. we are interested in a loop short-circuited to highlight the resonance phenomena relating to the geometric characteristics of the loop.

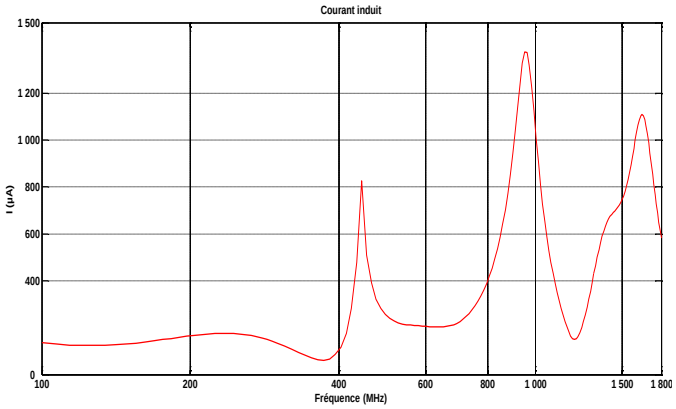

Fig.4: Courant induit sur la boucle 24x8 cm simulation par la MOM

We note on the fig.4 the presence of two very distinct zones. A first area in which the induced current remains virtually constant. It corresponds to frequencies whose wavelength is greater than about twice the perimeter of the loop.

Beyond these frequencies we observe the appearance of current peaks, showing that the rectangular loop resonates.

IV. Approach based on the Transmission Lines Theory (TLT)

To locate the resonances frequencies of the CI loop, we use the lines theory, with a few adjustments. Indeed the classical TLT calculates only currents of differential mode. This mode is present alone only two specific points, located in the centers of the side tracks of the loop (3 and 4). Elsewhere there is a superposition of a common mode and differential mode.

To integrate the common mode in the TLT, we decompose the incident excitation in two elementary excitations. The first consists to illuminating the loop by two identical waves coming from two opposite directions on part of the loop. These waves induce a pure common mode. The second is an illumination of the loop by two waves in phase opposition. It allows to excite a pure differential mode. Fig.5

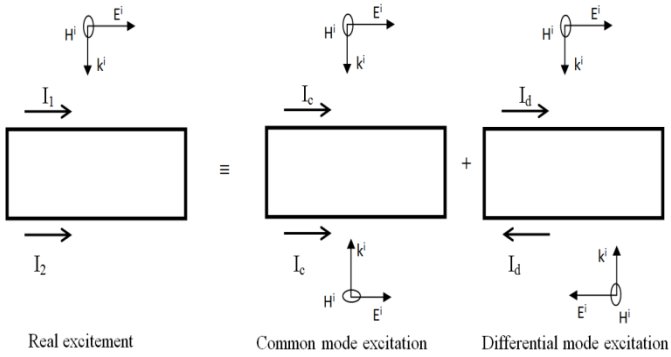

Fig.5: Decomposition of excitation in common and differential mode

Moreover, the TLT does not take account of lateral tracks of CI loops. Those above may have dimensions of the same order

of magnitude as the longitudinal slopes.

A possibility to account for the influence of lateral tracks was introduced by Degauque [7] and Zeddam [8]. It process a line of length (A + B) instead of (A). Parts (B) will of course be illuminated by the cross field Ex component as shown in the fig.6. While the tracks (A) are subject to the component Ez. In this figure we have chosen the origin of the orthonormal in the center of the longitudinal track 2 (z = 0).

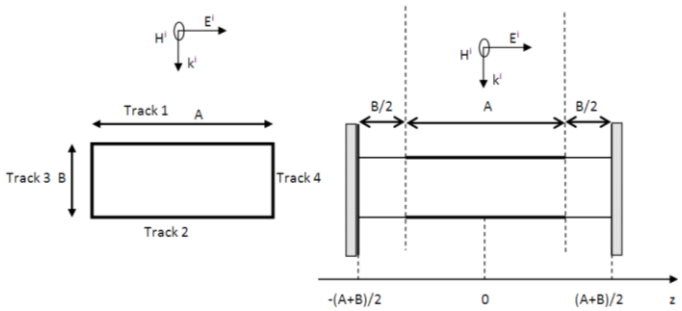

Fig.6: Integration of lateral tracks

A. Distribution of induced current by common mode

The two incident waves (Fig. 5), relating to excitation common mode induced on each element of length dz of longitudinal tracks 1 and 2 of the e.m.f of the same $de_c(z)$:

$$de_c(z) = \frac{E_{0z}^i}{2}\left(1 + e^{-j\beta B}\right)dz \qquad (7)$$

According to the orthonormal fig.6, sources equivalent to all these sources of elementary tension, brought to the middle of each track (at z = 0) are

$$e_c(z=0) = \int_{-A/2}^{0} de_c(z)e^{+j\beta z} + \int_{0}^{A/2} de_c(z)e^{-j\beta z} \qquad (8)$$

The integration is done only on the track whose length is A since for the incidence concerned, only that track is illuminated by the field Ez. The equivalent e.m.f at the center of track 1 and 2 is given by:

$$e_c(z=0) = \frac{E_{0Z}^i}{j\beta}\left(1 + e^{-j\beta B}\right)\left(1 - e^{-j\beta\, A/2}\right) \qquad (9)$$

This argument admits that the distribution of common mode current is symmetrical for the centers of tracks (z = 0), so it is zero at both ends $z = \pm\frac{A+B}{2}$ (Fig.6)

$$I_c\left(z = \pm\frac{A+B}{2}\right) = 0 \qquad (10)$$

The boundary condition (10) will be satisfied by the following distribution:

$$I_c(z) = A_c sin\left[\beta\left(\frac{A+B}{2} - |z|\right)\right] \qquad (11)$$

Similarly the condition (10) is fully equivalent to two runways open $z = \pm\frac{A+B}{2}$. By consequently, the loop of CI illuminated by a common mode excitation, z = 0 is equivalent to a generator of e.m.f. $e_c(z=0)$ given by equation (9), charged by A + B an impedance Z_{cor} which represents the corresponding open circuit $z = \pm\frac{A+B}{2}$ back to the centers of tracks 1 and 2. The equivalent circuit in the loop of CI, z = 0 is shown in fig.7.

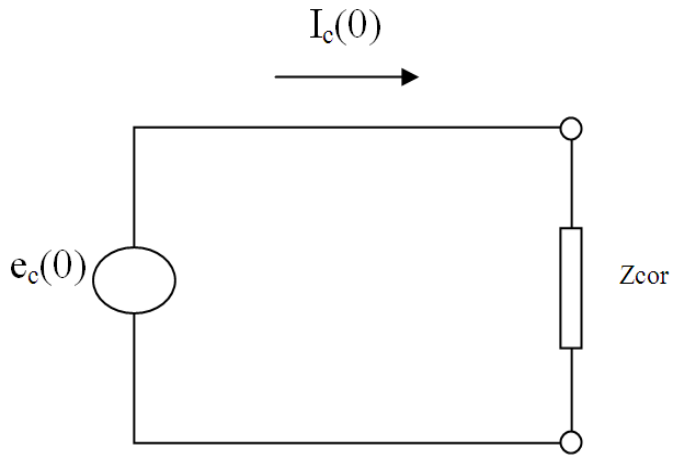

Fig.7: Equivalent circuit in common mode at z = 0

Z_{cor} The impedance is given by:

$$Z_{cor} = -jZ_c cotg\left(\beta\frac{A+B}{2}\right) \qquad (12)$$

The diagram of Fig.7, we can deduce the amplitude Ac of common mode

$$A_c = j\frac{e_c(0)}{Z_c \cos\left(\beta\frac{A+B}{2}\right)} \qquad (13)$$

B. Distribution of induced current by differential mode

The two incident waves (Fig. 5), relating to excitation of the differential mode, induced on each element of length dz of tracks 1 and 2 of the e.m.f of $de_d(z)$ identical modules, but in opposite phases:

$$de_d(z) = \frac{E_{0z}^i}{2}\left(1 - e^{-j\beta B}\right)dz \qquad (14)$$

We proceed in the same way as the common mode to infer the equivalent sources from all these sources of elementary tension reduced in the middle of each track (at z = 0):

$$e_d(z=0) = \frac{E_{0Z}^i}{j\beta}\left(1 - e^{-j\beta B}\right)\left(1 - e^{-j\beta\, A/2}\right) \qquad (15)$$

Contrary to common mode, differential mode current is maximum at both ends $z = \pm\frac{A+B}{2}$:

$$I_d\left(z = \pm\frac{A+B}{2}\right) = A_d \qquad (16)$$

The boundary condition (16) will be satisfied by the distribution of following current:

$$I_d(z) = A_d cos\left[\beta\left(\frac{A+B}{2} - |z|\right)\right] \qquad (17)$$

Similarly the condition (16) is equivalent to two tracks short-circuited $z = \pm\frac{A+B}{2}$.

Therefore, the equivalent circuit in the loop of CI, illuminated by a differential mode excitation, z = 0 is similar to fig.7. Except Zcor which is now replaced by Zccr:

$$Z_{ccr} = jZ_c tg\left(\beta\frac{A+B}{2}\right) \qquad (18)$$

From this same pattern, we can deduce the amplitude A_d of

the differential mode current:

$$A_d = -j\frac{e_d(0)}{Z_c \sin(\beta\frac{A+B}{2})} \quad (19)$$

The currents I_1 and I_2 induced on tracks 1 and 2 are calculated by superimposing the common mode currents (11) and differential mode (17):

$$I_1(z) = A_c sin\left[\beta(\frac{A+B}{2} - |z|)\right] + A_d cos\left[\beta(\frac{A+B}{2} - |z|)\right] \quad (20)$$

$$I_2(z) = A_c sin\left[\beta(\frac{A+B}{2} - |z|)\right] - A_d cos\left[\beta(\frac{A+B}{2} - |z|)\right] \quad (21)$$

The coefficients A_c and A_d take an infinite value only if:

$$Z_0 \cos\left(\beta\frac{a+B}{2}\right) = 0 \quad (22)$$

And

$$Z_0 \sin\left(\beta\frac{A+B}{2}\right) = 0 \quad (23)$$

- **Pour $Z_0 \cos\left(\beta\frac{A+B}{2}\right) = 0$**

$$\cos\left(\beta\frac{A+B}{2}\right) = 0 \quad (24)$$

$$\Rightarrow \beta\frac{A+B}{2} = (2N+1)\frac{\pi}{2} \quad (25)$$

with N=0, 1, 2,……..

$\beta = \omega\sqrt{\varepsilon\mu}$. We have considered the isolated loop, surrounded by air, so $\varepsilon_r = 1$ and $\beta = \omega\sqrt{\varepsilon_0\mu_0}$

$$\beta = \frac{\omega}{c} = \frac{2\pi f}{c}$$

(25) becomes: $\frac{2\pi f}{c}\frac{A+B}{2} = (2N+1)\frac{\pi}{2}$ (26)

Hence the resonant frequency common mode:

$$F_{Rc} = (2N+1)\frac{c}{2(A+B)} \quad (27)$$

- **for $Z_0 \sin\left(k\frac{A+B}{2}\right) = 0$**

$$\sin\left(k\frac{A+B}{2}\right) = 0 \quad (28)$$

$$\Rightarrow k\frac{A+B}{2} = N.\pi \quad (29)$$

With N=1, 2, 3,……..

(29) Becomes :

$$\frac{2\pi f}{c}\frac{A+B}{2} = N.\pi \quad (30)$$

Therefore the resonant frequency of the differential mode is:

$$F_{Rd} = N\frac{c}{(A+B)} = 2N\frac{c}{2(A+B)} \quad (31)$$

We therefore find the result observed in fig.4, which was obtained by the method of moments.

The resonance frequency of the loop can be easily linked to the length A and width B of the loop by the following approximate relation:

$$F_R = N\frac{c}{2(A+B)} \quad (32)$$

With c = 3108 m / s, speed of EM waves in vacuum and N=1, 2, 3, ...

V. Simulations and Measurements

The simulations were done under the MATLAB environment. The experimental validation was performed at the Laboratory LTPI / RUCI1 in Fez.

A. Achievement

We have made various prototypes of antennas as shown in Fig.8, using as the substrate, glass epoxy, type FR4 with relative permittivity εr = 4.32 and 1.53 mm thick.

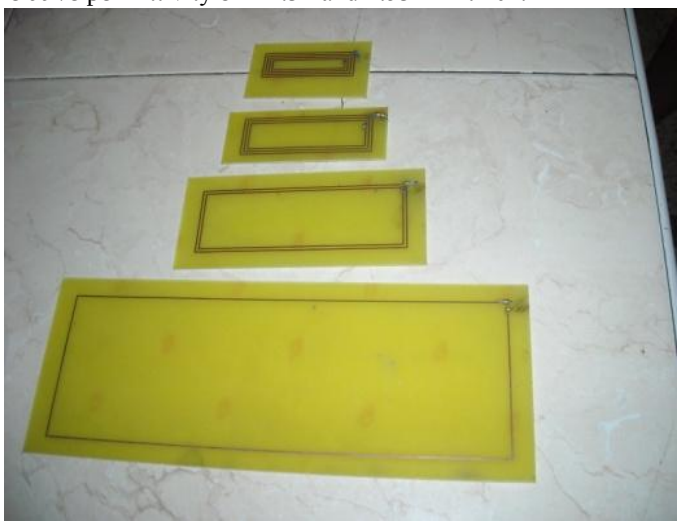

Fig.8: Antenna loops made

B. Measures and results

The coefficient of reflection of antennas made, were measured with a vector network analyzer HP-type operating in the100Hz-6000MHz band (Fig. 9).

Fig.9: Measurement of the reflection coefficient of the antenna using a vector network analyzer.

VI. Evaluation of Peaks and Frequency of Resonance of Induced Currents in Function of Geometric Characteristics of Printed Loop

The assessment of the size and position of resonance peaks of currents distributed on the printed tracks is crucial for designers of antennas tags. Indeed the action of these peaks

[1] Laboratory of Transmission and Processing of Information / Regional University Center interface

can completely change the normal operation of the transponder.

In this part the evolution of the amplitude of these peaks and their resonance frequency will be studied in function of geometric characteristics of loops.

A. Evaluation of the peaks as a function of the perimeter of the printed loop and the report (B / A)

In fig.10 we found the current to peak resonances for loops with different perimeters (from 40 cm to 120 cm) and reports Width / Length (B/A = 1/4, 1/3 and 2/5). We find in this figure a linear variation of these peaks as a function of the perimeter of these loops to the same ratio (B / A) thereof. Note that we have made loops whose resonant frequencies are between 400 MHz and 3 GHz.

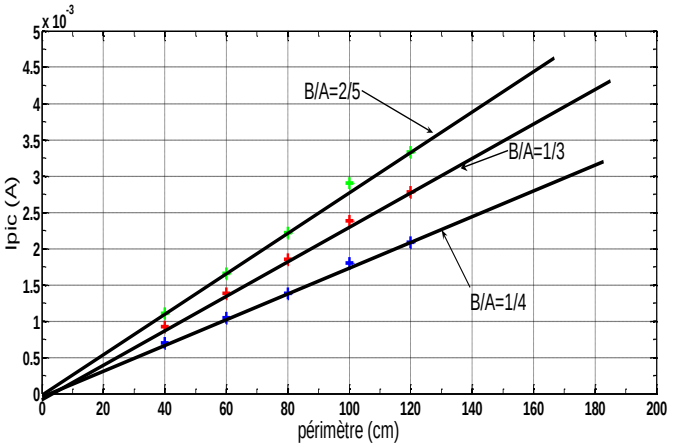

Fig.10: Amplitude of peak current at resonance for loops with different perimeters with a (B / A) constant

The peak current amplitude at resonance can be easily connected to the perimeter of the loop by the following equation:

$$I_{pic} = \alpha . P \quad (33)$$

With:

I_{pic} : The amplitude of peak current at resonance in (A).

α: The slope of the line in (A/m).

P: Scope of the loop in (m).

- For the $\frac{B}{A} = \frac{1}{4}$

$$\alpha_{\frac{1}{4}} = 1.735.10^{-3} = \frac{1}{4} \times 6.94.10^{-3} \quad (34)$$

- For the $\frac{B}{A} = \frac{1}{3}$

$$\alpha_{\frac{1}{3}} = 2.353.10^{-3} = \frac{1}{3} \times 6.94.10^{-3} \quad (35)$$

- For the $\frac{B}{A} = \frac{2}{5}$

$$\alpha_{\frac{2}{5}} = 2.776.10^{-3} = \frac{2}{5} \times 6.94.10^{-3} \quad (36)$$

From the above we can write α as follows:

$$\alpha_{\frac{B}{A}} = \frac{B}{A} \times K_t \quad (37)$$

With:

$K_t = 6.94.10^{-3}$ (A/m) (38)

The equation can be written as follows:

$$I_{pic\,\frac{B}{A}} = \frac{B}{A} \times K_t \times P \quad (39)$$

B. Evolution of the resonance frequencies of the induced currents in function of numbers of loops of rectangular spiral antennas (fixed perimeter).

The evaluation of the resonance peaks of currents on printed circuit tracks is crucial for designers of printed antennas. Indeed the action of these peaks can completely change the normal operation of the circuit.

We calculated the resonance frequency of the induced currents for four rectangular spiral antennas, respectively having a loop, two loops, three loops and four loops and the same perimeter 64cm, shown in Fig.11

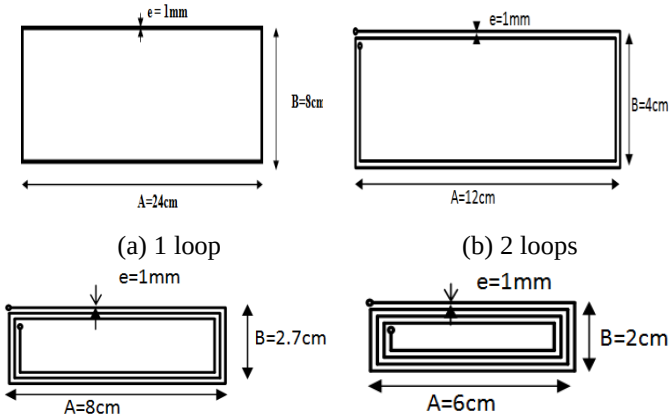

(a) 1 loop (b) 2 loops

(c) 3 loops (d) 4 loops

Fig.11: Dimensions of the Ics tracks used in the simulation and measurements

In fig.12 we observe that for the same scope the resonance frequencies of induced currents remain almost unchanged in function of the number of loops.

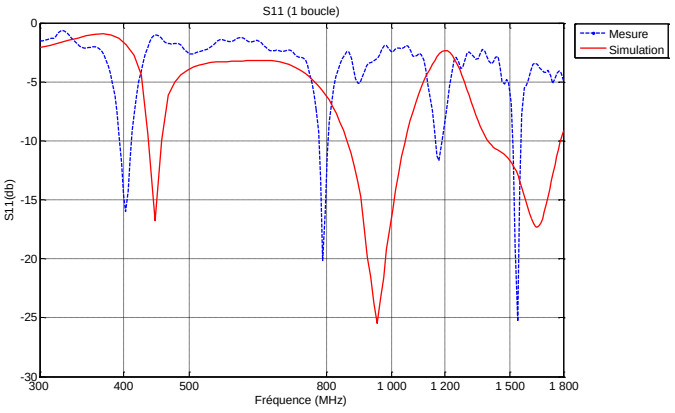

(a) 1 loop

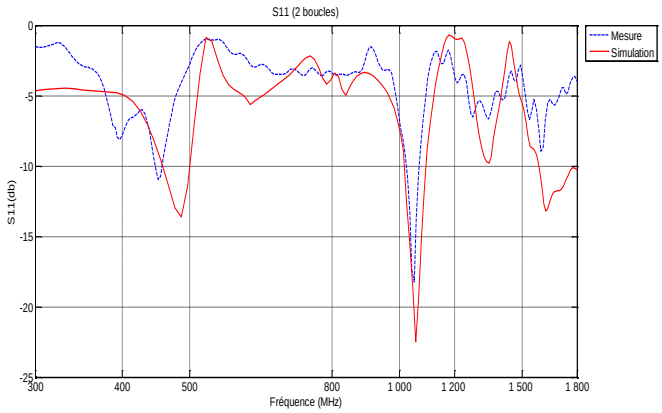

(b) 2 loops

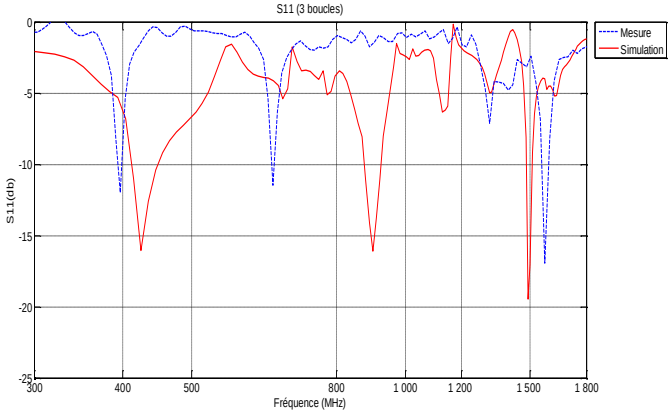

(c) 3 loops

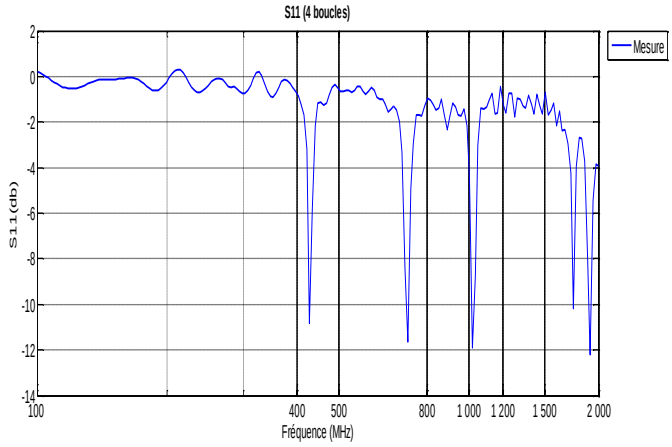

(d) 4 loops

Fig.12: Reflection coefficient S11 on the tracks of the ICs in fig.11-simulation by MOM and measurement

However, we notice a slight difference between the frequencies of resonance peaks of these antennas evaluated theoretically and those measured experimentally. This difference is surely due to the fact that in our theoretical model we do not take account of the dielectric permittivity of the substrate. Indeed, for the simulation we considered a spiral surrounded by air.

To account for the influence of the dielectric permittivity of the substrate on the positions of resonance frequencies, consider the case of a single loop. On Fig.13 we have ploted the S11 parameter for different values of ε_r substrate. We effectvely note that this setting actually influence the position of the resonance frequency.

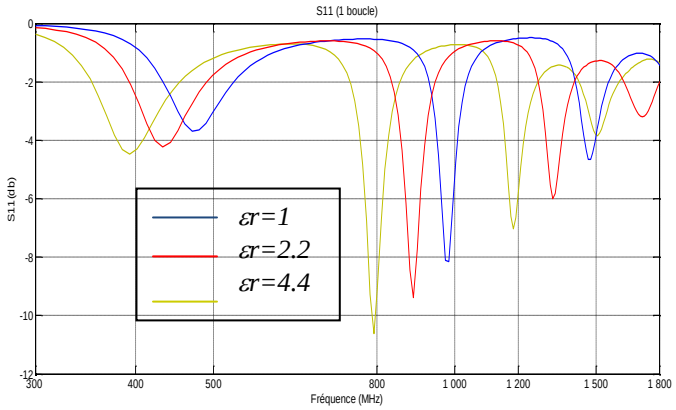

Fig.13 Influence of εr on peak resonances of spiral antennas

We can take advantage of this finding to try to design antennas that resonate at particular frequencies by playing on the nature of the dielectric substrates. This will allow the miniaturization of spiral antennas for RFID applications.

C. Evolution of the resonance frequencies of the induced currents in function of numbers of loops of rectangular spiral antennas (A and B fixed).

We have calculated the resonance frequencies of the induced currents for three rectangular spiral antennas, respectively having a loop, 2 loops and 3 loops and the same lengths (A = 24cm) and widths (B = 8cm): Fig.14

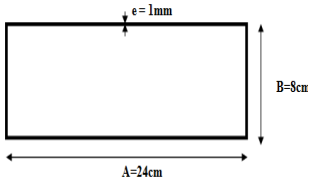

(a) 1 loop

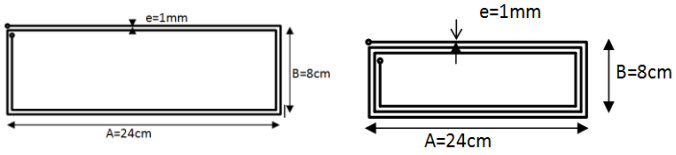

(b) 2 loops (c) 3 loops

Fig.14: Dimensions of tracks of printed antennas used in the simulation

On Fig.15 we see that for the same lengths (A = 24cm) and width (B = 8cm) resonance frequencies of the induced currents can be easily represented by the following approximate relation:

$$F_{R(N\ boucles\ )} = \frac{F_{R(1\ boucle\ )}}{N} \qquad (40)$$

With: N= 2, 3, 4, …

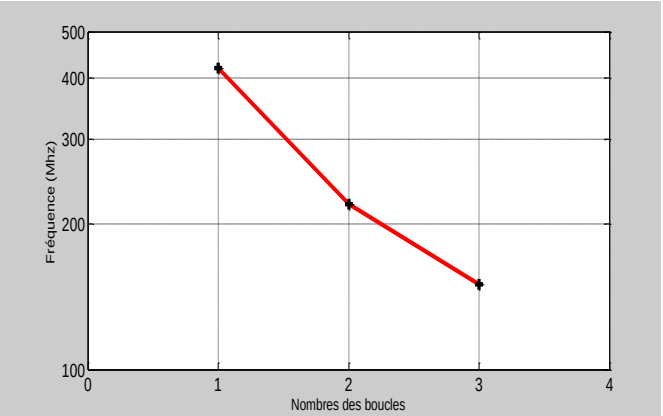

Fig.15: Frequencies of resonance in function of numbers of loops on the tracks of the ICs of the fig.14

VII. Conclusion

This paper presents the design of antennas for passive RFID tags. The first part concerned the quick introduction of this technology. It was followed by modeling of a spiral RFID UHF antenna using antenna theory.

Finally we have presented a simplified method of estimating the peak current and resonance frequencies of rectangular spiral RFID antennas.

This study shows that the amplitudes of peak's current resonances vary linearly as a function of geometrical characteristics of rectangular spiral antennas. This linearity can be used by designers of printed antennas to assess the amplitude of peaks current at resonance with simple graphs that can be drawn as a function of geometrical characteristics of loops. As well as resonance frequencies of induced currents are virtually unchanged in function of numbers of loops for the same perimeter.

Currently we are trying to establish a relationship between the resonance frequency of such antennas and the nature of the dielectric substrate on which it is printed. This will surely improve the performance of printed antennas and also contribute to their miniaturization.

References

[1] Klaus Finkenzeller, « RFID Handbook », Second Edition, John Wiley & Sons, Ltd, 2003.

[2] D. Bechevet, « Contribution au développement de tags RFID, en UHF et micro ondes sur matériaux plastiques », thèse doctorat de l'INPG, décembre 2005.

[3] S.Tedjini, T.P.Vuong, V. Beroulle, P. Marcel, "Radiofrequency identification system from antenna characterization to system validation", Invited paper, Asia-Pacific Microwave Conference, 15-18 december 2004, New Delhi, India.

[4] M. RIFI, «Modélisation du couplage électromagnétique produit par des champs transitoires sur des structures filaires et des pistes de circuits imprimés connectées à des composants non-linaires », thèse de Doctorat, Université Mohamed V, 1996.

[5] R.F.HARRINGTON, Field computation by Moment Methods, Mac Millman, 1968.

[6] M.OMID, Development of models for predicting the effects of electromagnetic interference on transmission line systems, PhD, University of Electro-Communications, Tokyo, Japan, 1997.

[7] P.DEGAUQUE et J.HAMELIN, Compatibilité Electromagnétique. Bruits et perturbations radioélectriques, Ed. Dunod 1990

[8] A.ZEDDAM, Couplage d'une onde électromagnétique rayonnée par une décharge orageuse à un câble de télécommunication, Thèse de Doctorat d'Etat, Lille 1988

El Mostafa MAKROUM Received his Bachelor of Computers Electronics Electrical Automatic from Faculty of Science and Technology, University Sidi Mohammed Ben Abdellah, Fez, Morocco, in 2003 and received the M.S. degree in 2007 Mohammadia School of Engineering, University Mohammed V, Rabat, Morocco. he is currently working towards the Ph.D. degree. His research interests the development of passive UHF RFID tags. He is particularly interested in their antennas.

Mounir RIFI is Professor in the Higher School of Technology, University Hassan II, Casablanca, Morocco. He received his Ph.D. degree from University of science and technology of Lille 1, France in 1987. His current research concerns Antennae, propagation and EMC problems.